

# The commonly used antimicrobial additive triclosan is a liver tumor promoter

Mei-Fei Yueh<sup>a</sup>, Koji Taniguchi<sup>b</sup>, Shujuan Chen<sup>a</sup>, Ronald M. Evans<sup>c</sup>, Bruce D. Hammock<sup>d,1</sup>, Michael Karin<sup>b</sup>, and Robert H. Tukey<sup>a,1</sup>

<sup>a</sup>Laboratory of Environmental Toxicology, Departments of Chemistry & Biochemistry and Pharmacology, and <sup>b</sup>Laboratory of Gene Regulation and Signal Transduction, Department of Pharmacology, University of California, San Diego, La Jolla, CA 92093; <sup>c</sup>Gene Expression Laboratory, Salk Institute for Biological Studies, La Jolla, CA 92037; and <sup>d</sup>Department of Entomology and Nematology and Comprehensive Cancer Center, University of California Davis Cancer Center, University of California, Davis, CA 95616

Contributed by Bruce D. Hammock, October 8, 2014 (sent for review June 17, 2014; reviewed by Christopher A. Bradfield and Margaret O. James)

Triclosan [5-chloro-2-(2,4-dichlorophenoxy)phenol; TCS] is a synthetic, broad-spectrum antibacterial chemical used in a wide range of consumer products including soaps, cosmetics, therapeutics, and plastics. The general population is exposed to TCS because of its prevalence in a variety of daily care products as well as through waterborne contamination. TCS is linked to a multitude of health and environmental effects, ranging from endocrine disruption and impaired muscle contraction to effects on aquatic ecosystems. We discovered that TCS was capable of stimulating liver cell proliferation and fibrotic responses, accompanied by signs of oxidative stress. Through a reporter screening assay with an array of nuclear xenobiotic receptors (XenoRs), we found that TCS activates the nuclear receptor constitutive androstane receptor (CAR) and, contrary to previous reports, has no significant effect on mouse peroxisome proliferation activating receptor  $\alpha$  (PPAR $\alpha$ ). Using the procarcinogen diethylnitrosamine (DEN) to initiate tumorigenesis in mice, we discovered that TCS substantially accelerates hepatocellular carcinoma (HCC) development, acting as a liver tumor promoter. TCS-treated mice exhibited a large increase in tumor multiplicity, size, and incidence compared with control mice. TCS-mediated liver regeneration and fibrosis preceded HCC development and may constitute the primary tumor-promoting mechanism through which TCS acts. These findings strongly suggest there are adverse health effects in mice with long-term TCS exposure, especially on enhancing liver fibrogenesis and tumorigenesis, and the relevance of TCS liver toxicity to humans should be evaluated.

triclosan | liver fibrosis | tumor promoter | hepatocellular carcinoma

Triclosan [5-chloro-2-(2,4-dichlorophenoxy)phenol, TCS] is a broad-spectrum antimicrobial agent ubiquitously used in personal care, household cleaning, and general consumer products (1). Originally developed in 1972 as an antibacterial component in a surgical scrub formulation, TCS is structurally similar to brominated diphenyl ethers, is generally accepted as well-tolerated and safe, and has become one of the most common additives to many consumer products, including disinfectants, soap, shampoo, detergent, toothpaste, mouthwash, deodorant, and even textiles. A substantial increase of TCS use has occurred during the last 20 y, resulting in widespread environmental pollution and its detection in waterways and the biological fluids of wild animals (2). In fact, TCS is listed among the seven most frequently detected compounds in streams across the United States, and ~1,500 tons continue to be produced annually worldwide (3). Once it has entered the body, TCS is mainly detoxified through glucuronidation by UDP-glucuronyltransferases (4). Recent studies have revealed that TCS is capable of interfering with various hormones as a weak endocrine disruptor in multiple species (5), as well as of impairing muscle contraction (6).

TCS was tested in several cell-based genotoxicity assays with no detectable mutagenic activity; nonetheless, the potential carcinogenicity of TCS in vivo has been largely unexplored. Previous animal data in rodents indicate that hepatocyte hypertrophy and vacuolization occurred after TCS ingestion, and

its action has been proposed to be mediated through peroxisome proliferation activating receptor  $\alpha$  (PPAR $\alpha$ ), a mode of action considered to be irrelevant to humans (2). To clarify the involvement of nuclear receptors, including PPAR $\alpha$ , in TCS-mediated responses, we first implemented a high-throughput xenobiotic nuclear receptor (XenoR) screening assay. Our studies indicate that PPAR activation is not relevant to the toxic effects of TCS in mice. However, long-term TCS treatment of mice led to hepatic cell proliferation, hepatocyte fibrosis, and oxidative stress. On the basis of the belief that liver fibrosis, when advanced, is a risk factor for developing hepatocellular carcinoma (HCC) (7), we also carried out a tumor promotion study in which TCS treatment was preceded by administration of a tumor initiator diethylnitrosamine (DEN). This study documents the molecular and biochemical events regarding TCS-mediated fibrogenesis and demonstrates that TCS acts as a promoter of HCC development. The mechanism of TCS-induced hepatic tumorigenesis in mice may be relevant to humans.

## Materials and Methods

**Animals.** Male C57BL/6 mice (3 wk old) were fed with a chow diet containing either 0.08% TCS ( $n = 6$ ) or no TCS ( $n = 6$ ). After 8 mo of TCS treatment, mice were killed and their livers were removed and were subject to analysis of gene expression and histological and immunochemical parameters. The Car-null ( $Car^{-/-}$ ) mouse line was a generous gift from Masahiko Negishi (National Institute of Environmental Health Sciences), and genotyping for Car-null mice was described previously (8). In the study of constitutive

## Significance

Triclosan [5-chloro-2-(2,4-dichlorophenoxy)phenol; TCS] is a broad-spectrum antimicrobial agent that has become one of the most common additives used in consumer products. As a result, TCS has significantly affected the environment and has been frequently detected in human body fluids. Through a long-term feeding study, we found that TCS enhances hepatocyte proliferation, fibrogenesis, and oxidative stress, which, we believe, can be the driving force for developing advanced liver disease in mice. Indeed, TCS strongly enhances hepatocarcinogenesis after diethylnitrosamine initiation, accelerating hepatocellular carcinoma (HCC) development. Although animal studies require higher chemical concentrations than predicted for human exposure, this study demonstrates that TCS acts as a HCC tumor promoter and that the mechanism of TCS-induced mouse liver pathology may be relevant to humans.

Author contributions: M.-F.Y., K.T., S.C., and R.H.T. designed research; M.-F.Y., K.T., and S.C. performed research; M.-F.Y., K.T., S.C., R.M.E., B.D.H., M.K., and R.H.T. contributed new reagents/analytic tools; M.-F.Y. analyzed data; and M.-F.Y., M.K., and R.H.T. wrote the paper.

Reviewers: C.A.B., University of Wisconsin–Madison; and M.O.J., University of Florida.

The authors declare no conflict of interest.

<sup>1</sup>To whom correspondence may be addressed. Email: rtukey@ucsd.edu or bdhammock@ucdavis.edu.

This article contains supporting information online at [www.pnas.org/lookup/suppl/doi:10.1073/pnas.1419119111/-DCSupplemental](http://www.pnas.org/lookup/suppl/doi:10.1073/pnas.1419119111/-DCSupplemental).

androstane receptor (CAR) activation, age-matched groups of 6–8-wk-old animals were used and treated i.p. every 24 h for 2 d with 50  $\mu$ L vehicle DMSO or TCS (15 mg/kg). After 48 h, the liver tissues were pulverized and used for preparation of cell lysate and total RNA. For the tumorigenesis study, C57BL/6 mice were bred with *Car*-null mice to generate *Car*<sup>+/-</sup> and *Car*<sup>-/-</sup> mice, and an approximately equal number of *Car*<sup>+/-</sup> and *Car*<sup>-/-</sup> mice were treated with a single i.p. injection of DEN (10 mg/kg) at the age of 15 d. These mice were divided into 3 groups ( $n = 30$ –35 for each group), control (containing both *Car*<sup>+/-</sup> and *Car*<sup>-/-</sup>), *Car*<sup>+/-</sup>-TCS, and *Car*<sup>-/-</sup>-TCS, and were treated with water (control) or 200 ppm TCS through drinking water. After 6 mo of treatment, all mice were killed, and their livers were removed, separated into individual lobes, and analyzed for the presence of HCC. Externally visible tumors ( $\geq 1$  mm) were counted and measured by stereomicroscopy. The large lobe was fixed in a 10% formalin phosphate buffer overnight and paraffin-embedded for subsequent H&E or specific immunohistochemistry staining. Remaining lobes were pulverized and frozen at  $-80^{\circ}\text{C}$  for total RNA isolation. All animals were housed at the University of California, San Diego, Animal Care Facility, and they received food and water ad libitum. All animal use protocols, mouse handling, and experimental procedures were approved by the University of California, San Diego, Animal Care and Use Committee, and these protocols were conducted in accordance with federal regulations.

**Xenobiotic Receptor Screening Assay.** The activity of mouse XenoRs, including pregnane X receptor (PXR), CAR, liver X receptor  $\alpha$  (LXR  $\alpha$ ), farnesoid X receptor (FXR), vitamin D receptor (VDR), PPAR $\alpha$ , PPAR $\beta$ , PPAR $\gamma$ , estrogen receptor  $\alpha$  (ER $\alpha$ ), ER $\beta$ , and glucocorticoid receptor (GR) in response to TCS (10  $\mu$ M) was monitored. CV-1 cells were maintained in DMEM (Life Technologies) supplemented with 10% FBS, seeded in 96-well plates, and transfected with an expression vector containing a specific nuclear receptor (i.e., PXR, CAR, LXR $\alpha$ , VDR, FXR, PPAR $\alpha$ , PPAR $\beta$ , PPAR $\gamma$ , or GR) and RXR, along with a luciferase reporter containing the appropriate DNA response element, as described previously (9). The assay was first validated with known nuclear receptor ligands as positive controls, including pregnenolone 16 $\alpha$ -carbonitrile (10  $\mu$ M; Sigma) for PXR, 1,4-bis-[2-(3,5-dichloropyridyloxy)]benzene (250 nM; Sigma) for CAR,  $\beta$ -estradiol (10 nM; Sigma) for ER, T0901317 (1  $\mu$ M; Cayman Chemical) for LXR $\alpha$ , calcipotriol (10  $\mu$ M; Sigma) for VDR, GW4064 (1  $\mu$ M; Sigma) for FXR, WY14643 (30  $\mu$ M; Sigma) for PPAR $\alpha$ , GW501516 (100 nM) for PPAR $\delta$ , rosiglitazone (1  $\mu$ M; Cayman Chemical) for PPAR $\gamma$ , and dexamethasone (100 nM; Sigma) for GR. For the CAR ligand-binding assay, CV-1 cells were transiently transfected with the expression vector containing the Gal4 DNA-binding domain fused with the ligand-binding domain of murine or human CAR and cotransfected with the luciferase reporter plasmid, mh 100-luc (10). The day after the transfection, the positive compound of each nuclear receptor or TCS was added and the cells were incubated for an additional 24 h. The luciferase activities were measured and normalized by  $\beta$ -gal activity.

**Reverse Transcription and Real-Time PCR.** The mRNA from fresh frozen tissues was extracted using TRIzol (Life Technologies) according to the manufacturer's protocol. cDNA was prepared using iSCRIPT (BioRad), and real-time PCR was performed using SYBR master mix (SsoAdvanced SYBR supermix, BioRad) with a pair of gene-specific primers and the cyclophilin (CPH) gene as an internal control gene, using the CFX96 Touch Real-Time PCR Detection System (BioRad). Each sample was performed in triplicate, normalized to the internal control gene CPH, and quantitated on the basis of the formula  $\Delta\text{Ct} (\text{cycle threshold}) = \text{Ct}(\text{tested gene}) - \text{Ct}(\text{CPH})$ . The mouse sequences for forward and reverse primers are listed in Table S1.

**Immunohistochemical Staining, Sirius Red Staining, BrdU incorporation, in Situ Detection of Superoxide, and TUNEL Assay.** For the staining of  $\alpha$ -fetoprotein (Biocare, Catalog no. CP028A), Ki-67 (GeneTex, Catalog no. GTX16667),  $\alpha$ -smooth muscle actin ( $\alpha$ -SMA) (Abcam, Catalog no. ab5694), and CD45 (GeneTex, Catalog no. GTX76582), paraffin liver sections were prepared in the Histology Core (University of California, San Diego). Formalin-fixed, paraffin-embedded liver slides were deparaffinized and rehydrated, using xylene followed by alcohol and PBS washings. Antigen retrieval of tissue slides and the immunohistochemical staining with a primary antibody, secondary biotinylated antibody, and streptavidin-HRP (Pharmingen) were achieved as described previously (11). Hepatic collagen content was analyzed by Sirius red staining (saturated picric acid containing 0.1% Sirius Red F3B) of paraffin-embedded sections to assess the degree of fibrosis. The Sirius red-positive area was measured in four individual fields on each slide and quantified using NIH imaging software. For BrdU staining, vehicle- or TCS-treated mice were i.p. injected with 0.1 mL BrdU (10 mg/mL, Sigma) and killed 3 h later. Livers

were removed and processed as indicated earlier. Paraffin-embedded sections were stained using the BrdU In-Situ Detection Kit (BD Biosciences). Dihydroethidium (DHE; Sigma) staining was performed to examine the accumulation of superoxide anions. Briefly, liver sections were embedded in Optimum Cutting Temperature embedding compound, and the frozen liver sections, after cryosectioning, were incubated with 5  $\mu$ M dihydroethidine hydrochloride (Sigma) for 30 min at  $37^{\circ}\text{C}$  and were observed under a fluorescence microscope. Superoxide detection was also carried out with primary hepatocytes (12) after TCS (20  $\mu$ M) treatment. Detection of apoptotic cells in tissue sections was performed by the TUNEL assay with the In-Situ Cell Death Detection Kit (TMR red, Roche), according to the protocol described previously (11). TUNEL-positive cells were counted on five fields of 200 $\times$  magnification per slide.

**Alanine Aminotransferase Assay and Cell Proliferation Analysis.** Mouse blood was collected at the end of the 6-mo treatment in the tumorigenesis study. Alanine aminotransferase (ALT) activity was determined by the Infinity ALT [glutamate pyruvate transaminase (GPT)] Kit (Thermo), and ALT standards (Enzyme Linearity Test Set) were from Microgenics CASCO. Cell proliferation was determined by an MTT [3-(4,5-dimethylthiazol-2-yl)-2,5-diphenyltetrazolium bromide] assay. Human hepatoma (HepG2) cells plated at  $5 \times 10^4$  cells per well in a 96-well microplate were treated with TCS (15  $\mu$ M) for 24 h, followed by the addition of 50  $\mu$ L per well of 5 mg/mL MTT solution and incubation for 2 h. Subsequently, the MTT solution was replaced by 250  $\mu$ L dimethyl sulfoxide. The absorbance was measured by 540 nm with a microplate reader (Biorad).

**Statistical Analysis.** Prism software (Version 5, GraphPad) was used to analyze the data, which are presented as mean  $\pm$  SD. Differences between two groups were compared using the two-tailed unpaired Student *t* test. Differences among multiple groups were compared using one-way analysis of variance. *P* values  $< 0.05$  were considered statistically significant, and statistically significant differences are indicated with \**P*  $< 0.05$ ; \*\**P*  $< 0.005$ ; \*\*\**P*  $< 0.0005$ .

## Results

**TCS Treatment Increases Hepatocyte Proliferation and Induces Liver Fibrosis and Reactive Oxygen Species Accumulation.** In agreement with its abilities to induce hepatocyte hypertrophy and proliferation in rodent livers (2), TCS exposure for 8 mo resulted in an increased liver-to-body weight ratio without affecting body weight (Fig. 1A). Real-time PCR analysis revealed TCS-induced expression of several markers and genes, including *Ki-67*, *c-Myc*, and *Cyclin D1*, which are all relevant to regulation of DNA synthesis and cell proliferation (Fig. 1B). Enhanced cell proliferation was also indicated by the MTT cell proliferation assay in HepG2 cells treated with TCS (Fig. 1C). Elevated expression of *Ki-67* and cyclin D1 is associated with the onset of hepatocyte DNA replication in rodent models of liver regeneration (13). The TCS-induced proliferative response was associated with increased expression of fibrogenic genes *collagen 1a1*,  $\alpha$ -*Sma*, and *tissue inhibitor of metalloproteinase 1* (*Timp1*) (Fig. 1D). TCS-treated mice also exhibited elevated collagen accumulation in liver detected by Sirius red staining, further demonstrating the occurrence of hepatic fibrosis (Fig. 1E). One pathogenic mechanism associated with fibrosis is oxidative stress (14). We assessed accumulation of hepatocyte superoxides by staining frozen liver sections with DHE, the oxidation of which gives rise to the fluorescent derivative ethidine. Increased levels of superoxide were observed in livers of TCS-treated mice (Fig. 1F). Moreover, TCS-treated livers exhibited a marked increase in expression of oxidative stress-responsive genes, including *heme oxygenase 1*, *NADPH hydrogenase quinone 1*, and *GST* (Fig. 1G), indicating occurrence of oxidative stress (15). Collectively, these data indicate that TCS exposure creates a prooxidant hepatic environment and has proliferative and profibrogenic effects.

**Nuclear Receptor Activation by TCS.** Liver fibrosis during chronic liver disease is believed to promote hepatic carcinogenesis (7). Before testing the hypothesis, that the profibrogenic effect of TCS would ultimately lead to liver carcinogenesis, we examined whether TCS activates PPAR $\alpha$ , as previously suggested (2). We monitored activities of a series of mouse XenoRs, including PXR, CAR, LXR $\alpha$ , FXR, VDR, PPAR $\alpha$ , PPAR $\beta$ , PPAR $\gamma$ , ER $\alpha$ , ER $\beta$ , and GR, and validated the assay by using a positive ligand

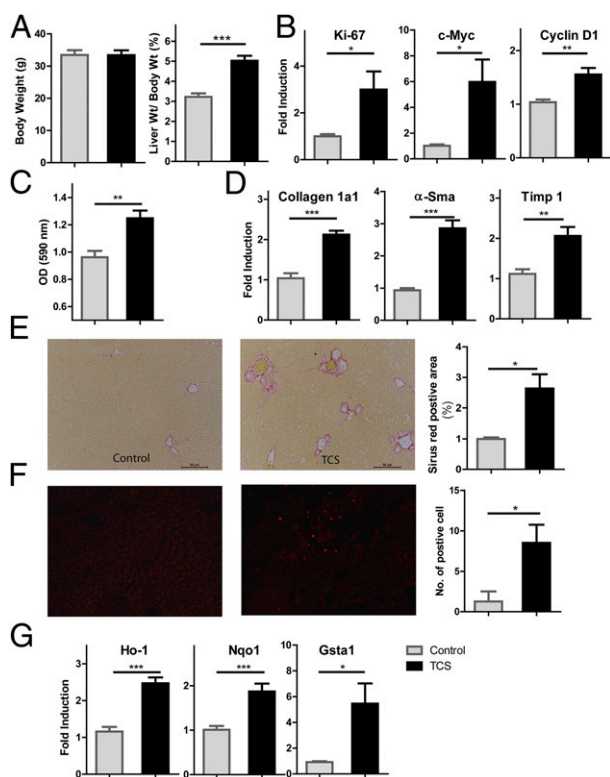


**Fig. 1.** TCS treatment resulted in cell proliferation and fibrogenesis, accompanied by generation of ROS. Male mice were fed with a chow diet containing either 0.08% TCS or no TCS for 8 mo. (A) Body weight and liver weight (expressed as a percentage of body weight) were compared between control ( $n = 6$ ) and TCS-treated ( $n = 6$ ) mice. (B) Expression of genes *Ki-67*, *c-Myc*, and *Cyclin D1* was quantitated using real-time PCR. (C) The cell proliferation of HepG2 cells after TCS treatment (15  $\mu$ M) was examined by an MTT assay. (D) Expression of genes *Collagen 1a1*,  *$\alpha$ -Sma*, and *Timp 1* associated with liver fibrosis was analyzed by real-time PCR. (E) (Left) Representative Sirius red staining of liver sections shows collagen deposition, indicating fibrosis progression in TCS-treated mice compared with control mice. (Right) The quantitation of the collagen-positive area. (F) (Left) Liver cryosections were incubated with 5  $\mu$ M DHE for 30 min at 37  $^{\circ}$ C. (Right) In situ detection of superoxides in the liver sections was quantitated by counting positive cells in four different fields, using a fluorescence microscope. (G) Real-time PCR analysis for oxidative stress response genes *heme oxygenase 1* (*Ho-1*), *NADPH hydrogenase quinone 1* (*Nqo-1*), and *GST* (*Gsta1*).

for each nuclear receptor, as detailed previously (9). Of the 11 XenoRs screened with TCS (10  $\mu$ M), only CAR was modestly activated by TCS (Fig. 2A). All other XenoRs displayed statistically insignificant activation, including PPAR $\alpha$ , which was previously suggested to be responsible for TCS-mediated hepatocyte proliferation and hypertrophy (2). To characterize CAR activation by TCS, we examined TCS effect on a fusion protein containing the mouse CAR-ligand binding domain and the Gal4 DNA-binding domain. We found that the positive controls 1,4-bis[2-(3,5-dichloropyridyloxy)] benzene (TCPOBOP) and 6-(4-chlorophenyl)imidazo[2,1-b][1,3]thiazole-5-carbaldehyde-O-(3,4-dichlorobenzyl)oxime (CITCO) elicited a robust induction for mouse and human CARs, respectively, whereas TCS treatment had an insignificant effect on either of the CARs (Fig. 2B), indicating that TCS is a CAR activator, but not a direct ligand for either mouse or human CAR (Fig. 2B). The expression of *Cyp2b10*, a gene target that is regulated by CAR, was highly induced by TCS exposure, whereas a nearly complete absence of *Cyp2b10* gene induction was observed in *Car*<sup>-/-</sup> mice after TCS treatment, indicating that CAR activation by TCS is responsible for induction of the *Cyp2b10* gene. Consistent with the transcript levels, the Cyp2b10 protein was induced by TCS treatment, and

the induction was blocked in *Car*<sup>-/-</sup> livers (Fig. 2C). These results indicate that TCS does not activate PPAR $\alpha$ , although it activates CAR through an indirect mechanism.

**TCS Acts as a Tumor Promoter in Liver Carcinogenesis.** There are two things that prompted us to examine the effect of TCS on liver tumorigenesis: first, the fibrogenic and proliferative potential after TCS exposure, and second, previous literature that established that CAR activation by phenobarbital and similar inducers can promote liver carcinogenesis (16–18). Previous studies have shown that a single postnatal injection of tumor initiator DEN, which induces hepatocyte DNA damage and oncogenic mutations (19), can result in the development of HCC. On the basis of the fact that male mice are more sensitive than females to DEN-induced tumorigenesis (20), male mice were given a single injection of DEN, followed by TCS treatment in drinking water (200 ppm) for 6 mo ( $n = 30$ –35 in each group). TCS treatment significantly increased liver tumorigenesis, but its action seemed to be independent of the nuclear receptor CAR (Fig. 3A). TCS-treated mice had a higher tumor number, bigger tumor size, and greater tumor incidence than mice given DEN alone, whether

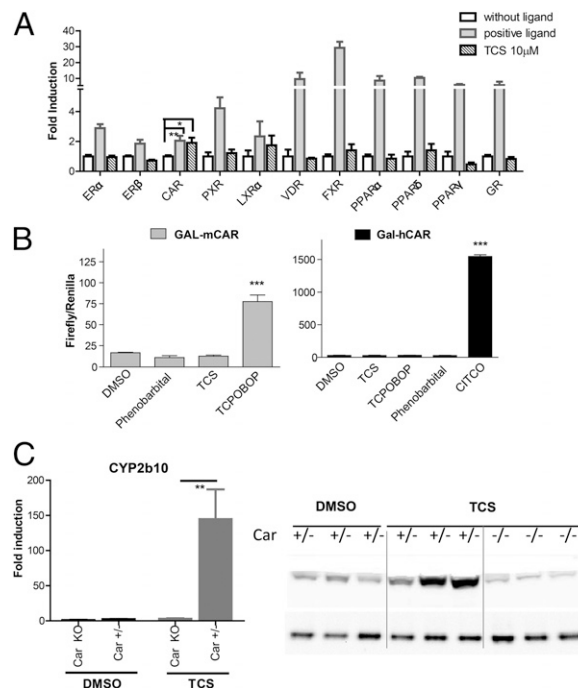


**Fig. 2.** Xenobiotic receptor activation profile of TCS. (A) Xenobiotic receptor screening assay was performed to test for TCS activity toward activation of PXR, CAR, LXR $\alpha$ , FXR, VDR, PPAR $\alpha$ , PPAR $\beta$ , PPAR $\gamma$ , ER $\alpha$ , and ER $\beta$ . Transfection experiments were conducted according to the descriptions in *Materials and Methods*. Luciferase activity was represented as fold induction relative to DMSO-treated cells. The results are expressed as the mean  $\pm$  SD; \* $P < 0.05$ . (B) The CAR ligand binding assay was performed by transfecting HepG2 cells with the expression vector containing the Gal4 DNA binding domain fused with the ligand-binding domain of (Left) murine CAR (mCAR) or (Right) human CAR (hCAR) and the luciferase reporter plasmid mh100. After transfections, cells were treated for 24 h with phenobarbital (1 mM), TCS (10  $\mu$ M), TCPOBOP (25  $\mu$ M), or CITCO (10  $\mu$ M). Firefly luciferase activity was measured and normalized by using the level of *renilla* luciferase activity. (C) (Left) Age-matched heterozygous (*Car*<sup>+/-</sup>) and *Car*-null mice (*Car*<sup>-/-</sup>) ( $n = 3$ ) were treated with either DMSO or TCS (15 mg/kg) by intraperitoneal injection for 48 h. The liver tissues from each group were dissected, pulverized with liquid nitrogen, and pooled together. Total RNA was prepared followed by cDNA synthesis, and real-time PCR for *Cyp2b10* expression was conducted to determine the Ct value, with cyclophilin as an internal control gene. (Right) The microsomal proteins were prepared from liver tissues and subject to Western blot analysis, using Cyp2b10 antibody as the primary antibody.



they were heterozygous *Car* ( $Car^{+/-}$ ) or homozygous null  $Car^{-/-}$  mice, although the exception is that the tumor number in  $Car^{+/-}$  mice is approximately twice as large as that in  $Car^{-/-}$  mice. Strikingly, the number of detectable HCCs was ~4.5-fold higher in TCS-treated mice than in control mice. Approximately 25% of DEN-only mice exhibited small nodules, whereas more than 80% of TCS-treated mice developed tumors. Maximal tumor diameter was also 3.5-fold larger in TCS-treated mice (Fig. 3A). In addition, many HCCs in TCS-treated mice exhibited signs of neovascularization (indicated by the arrow in Fig. 3B). As a consequence, TCS-treated mice exhibited increased serum levels of ALT and histological alterations in hepatocytes, suggesting that exposure to TCS is responsible for liver injury that leads to disrupted liver integrity and compromised liver function (Fig. 3B). Expression of  $\alpha$ -fetoprotein (AFP), a clinical biomarker for HCC, was noticeably elevated in the TCS-treated livers, as detected by immunostaining and real-time PCR (Fig. 3C), further supporting the malignant potential of tumors in TCS-treated mice. Expression of fetal-specific liver genes, including *insulin-like growth factor 2* and *delta-like 1 homolog*, was dramatically induced in TCS-treated livers (Fig. 3C). These results collectively demonstrate that TCS treatment increases susceptibility to DEN-induced carcinogenesis and promotes HCC development.

**Characteristics of Tumor-Bearing Livers in TCS-Treated Mice.** To further characterize livers of mice that underwent DEN initiation followed by a 6-mo TCS treatment, we examined cell proliferation and fibrogenesis. Our results show that when comparisons were made between TCS and control mice, TCS exposure enhanced hepatocyte proliferation and exerted profibrogenic effects in the

liver. Labeling with BrdU and expression of Ki-67 revealed more proliferating hepatocytes in TCS-treated mice (Fig. 4A and B). Furthermore, TCS-treated mice exhibited collagen deposition and increased  $\alpha$ -Sma expression, as detected by Sirius red staining and immunostaining, respectively (Fig. 4C and D); real-time PCR analysis also showed elevated expression of genes associated with liver fibrosis, including *collagen 1a1*,  $\alpha$ -Sma, and *Timp1* (Fig. 4E), indicating the occurrence of liver fibrogenesis.

**Proinflammatory Responses Are Induced by TCS Treatment.** Human and animal studies suggest that hepatic immunity is altered and liver inflammation is elevated during liver fibrosis (21, 22). We determined that the abundance of inflammatory intrahepatic leukocytes (Cd45<sup>+</sup>) in the fibrogenic liver of TCS-treated mice was greatly increased (Fig. 5A). In the presence of TCS, mice exhibited an increase in liver inflammation, as shown by consistently induced levels of chemokine (C-X-C motif) ligand 2 (CXCR2), a cytokine associated with histological liver lesions, tumor angiogenesis, and metastatic potential (23, 24). Moreover, the hepatic expression of the inflammatory cytokines TNF $\alpha$ , and IL-6, as well as the fibrogenic cytokine TGF $\beta$ , was increased in mice receiving TCS compared with controls (Fig. 5B). Under the TCS-mediated proinflammatory and profibrogenic environment, more apoptotic hepatocytes were detected (Fig. 5C). When primary hepatocytes were treated with TCS, superoxides were detected by DHE staining (Fig. 5D). NADPH oxidase, which converts molecular oxygen to superoxide, has been associated with reactive oxygen species (ROS) generation and liver injury (25). We examined gene expression levels of various NADPH oxidase subunits, and up-regulation of *gp91phox*, *p47phox*, and *p67phox* mRNAs was observed in livers of TCS-treated mice (Fig. 5E), suggesting *gp91phox* may be a contributing factor in superoxide generation. Together, these results demonstrate that TCS-treated mice exhibited hepatocyte death, compensatory proliferation fibrogenesis, oxidative stress, and proinflammatory responses, a critical process in hepatocarcinogenesis (26).

## Discussion

The human health effects resulting from long-term exposure to daily use of TCS-containing products and from environmental contamination are unknown. Several studies have found TCS in urine, serum, and breast milk in a high percentage of the population, indicating widespread TCS exposure. TCS levels in serum and urine varied greatly among people and can reach as high as 354 and 3,790  $\mu$ g/L, respectively, largely depending on the regular use of TCS-containing products (27). Another important factor is that individual metabolic capacity (e.g., UDP-glucuronyltransferase 1 expression levels affected by liver function or genetic polymorphism) may largely affect TCS concentration in the body. In our first long-term TCS study, mice received ~68.6 mg/kg TCS daily, based on a diet of 3 g daily chow. For the tumorigenesis study, mice received less than 28.6 mg/kg TCS daily through water, based on 5 mL daily water consumption and because of partial solubility of TCS at a concentration of 200 ppm. To put this into perspective, people are exposed to ~0.05 mg/kg of TCS using 1 g of toothpaste that contains 0.3% TCS when brushing their teeth, although the majority of the toothpaste would go down the drain a few minutes afterward. To date, it is challenging to use yet-to-be-defined relevant levels of TCS in animal studies and to translate findings to human health. We took a logical first step by conducting a mechanism-based study in mice that defines the pathological condition in the liver elicited by TCS exposure. With these scientific bases, longitudinal epidemiology studies examining the correlation of TCS body concentrations and liver disease should be carried out in the future.

Diseases leading to liver fibrosis include alcoholic-induced liver disease, viral hepatitis B and C, nonalcoholic steatohepatitis, and biliary disease (28). Our findings suggest it would be meaningful to evaluate whether long-term TCS exposure may also be a risk factor for developing liver fibrosis in humans. In mice, we find that TCS administration causes chronic liver damage and apoptosis.

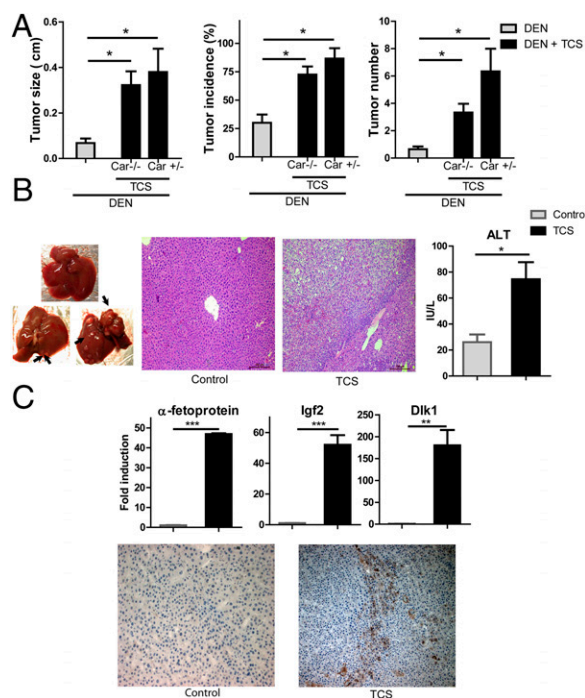


**Fig. 3.** TCS-mediated tumorigenesis after DEN injection. (A) A 6-mo TCS treatment increases DEN-induced tumor development. Maximal tumor sizes (diameters), tumor incidence (%), and numbers of tumors ( $\geq 1$  mm) in livers of control, TCS- $Car^{+/-}$ , and TCS- $Car^{-/-}$  mice 6 mo after injection of a dose of DEN (10 mg/kg) at the age of 15 d; \* $P < 0.05$  vs control mice. (B) (Left) Livers of 6.5-mo-old male control (Top) and TCS-treated (Bottom) mice. Arrowheads indicate neovascularization. (Middle) Histological analysis with H&E staining. (Right) Serum ALT levels. (C) (Top) Effects of TCS on expression of fetal-specific liver genes. RNA from control and tumor-bearing livers from TCS-treated mice were analyzed by real-time PCR. (Bottom) Expression of  $\alpha$ -fetoprotein in liver sections was immunostained with the anti-AFP antibody.

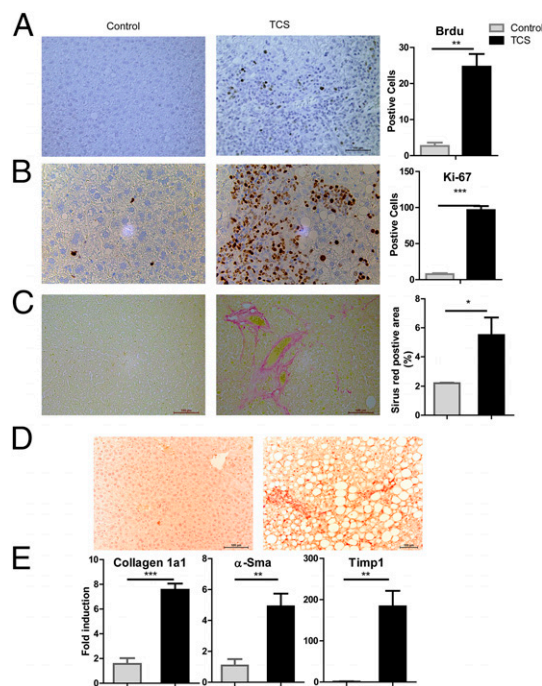


**Fig. 4.** TCS-induced hepatocyte proliferation and fibrogenesis in the tumorigenesis study. (A) (Left) Hepatocyte proliferation was measured by BrdU incorporation 48 h after injection. (Right) Quantitation by counting the number of BrdU-positive nuclei per ~500 hepatocytes. (B) (Left) The extent of liver cell proliferation was also determined by Ki-67 immunostaining. (Right) Quantitation of Ki-67-staining positive cells. (C–E) The extent of fibrosis was investigated by Sirius red staining (C) and by detecting fibrogenic parameters, including  $\alpha$ -SMA expression detected by immunostaining (D) and gene expression of *Collagen 1a1*,  $\alpha$ -Sma, and *Timp1*, detected by real-time PCR (E).

With their regenerative capacity, the surviving hepatocytes undergo compensatory proliferation and fibrogenesis. In our tumorigenesis study, we further demonstrated that TCS markedly increased animals' susceptibility to tumorigenesis, supporting the belief that fibrosis, when advanced, is a risk factor for developing HCC (7, 29). Our results suggest that TCS-induced hepatocyte proliferation and fibrogenesis may be the major driving force responsible for the etiology of HCC development.

Profibrogenic mediators elicited by TCS exposure remain to be explored. The most common and relevant mechanisms that are recognized in hepatic fibrogenesis are the production of ROS (30) and recruitment of inflammatory cells (31), both of which were observed in the livers of TCS-treated mice. ROS generation in alcohol abuse, HCV infection, and chronic cholestasis is associated with various types of liver injuries accompanied by hepatic fibrosis (14). In the TCS-treated mice, hepatic collagen deposition is concomitant with signs of oxidative stress. Activation of the NADPH oxidase also supports the notion that TCS creates a prooxidant hepatic environment that contributes to liver pathogenesis. The compelling evidence linking NADPH oxidase to liver fibrogenesis is that mice lacking p47phox are protected from developing liver fibrosis after chronic liver injury after bile duct ligation (32). It will be interesting to understand the mode of activation through which TCS induces gp91phox expression. We believe that an increased susceptibility to oxidative stress may sustain, at least in part, fibrosis observed in TCS-treated mice because oxidative-related molecules may act as mediators to modulate tissues and cellular events responsible for the progression of liver fibrosis (33). Tsukamoto and colleagues (34) demonstrated that ROS levels were positively associated with the release of TNF $\alpha$  and IL-6 in Kupffer cells. These results coincide with increased expression of TNF $\alpha$  and IL-6 in the livers of TCS-treated mice, suggesting that activation of inflammatory cells may

represent a major source of oxidative stress-related molecules that subsequently mediate cytotoxic responses and profibrogenic effects. Many questions regarding TCS-mediated fibrosis need to be further explored. For example, the relationship of TCS-induced liver fibrogenesis to the role played by hepatocytes, Kupffer cells, endothelial cells, and stellate cells is currently unclear. Animal and clinical studies indicate that hepatic stellate cells play a central role in fibrogenesis, are principal matrix-producing cells, and express  $\alpha$ -SMA when activated. In the livers of TCS-treated mice, elevated levels of  $\alpha$ -Sma and an increase in collagen deposition imply activation of hepatic stellate cells. Increased expression of inflammatory cytokines, such as CXCR2 and TNF $\alpha$ , as detected after TCS treatment, is associated with activation of Kupffer cells (35), which represent another potential target to TCS insult. TCS proliferative and profibrotic property may not be restricted in the liver: Our preliminary data show that 8.3% of mice exposed to TCS developed renal hypertrophy with increases in renal cell proliferation and collagen accumulation, indicating the occurrence of kidney fibrogenesis (Fig. S1). It is worthwhile exploring the possibility of TCS causing fibrotic disease to other organs and finding the central mediators that dictate fibrogenesis in these organs.

In our nuclear receptor assay, mouse PPAR displayed insignificant activation with 0.86-fold induction (compared with DMSO as 1-fold) in response to TCS. This experiment was validated by using WY14643 (30  $\mu$ M), a known PPAR $\alpha$  ligand, which gave rise to an 8.6-fold induction for PPAR $\alpha$  activation. These results do not support the previous belief that TCS exerts its

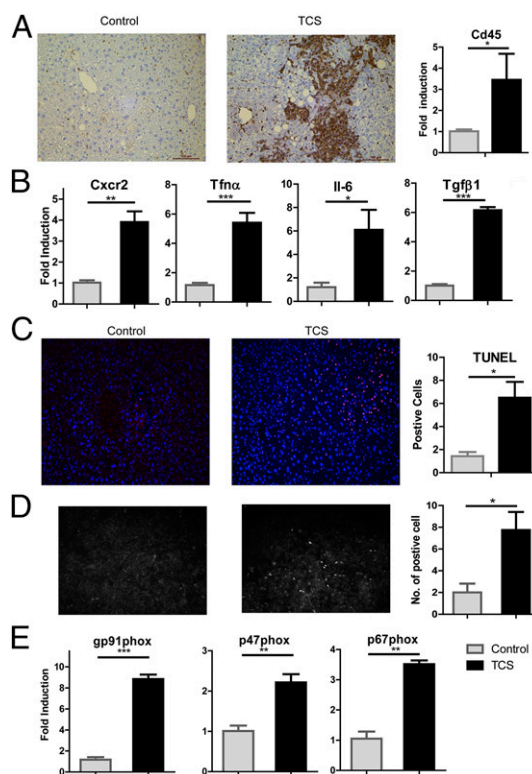


**Fig. 5.** Activation of inflammatory responses and NADPH oxidase in livers of TCS-treated mice. (A) Expression of Cd45 was immunostained with the anti-Cd45 antibody in liver sections and quantitated by real-time PCR. (B) Hepatic expression of *Ccr2* and inflammatory genes, including *Tnf $\alpha$* , *Il-6*, and *Tgf $\beta$ 1*, was quantitated by real-time PCR. (C) Liver cell apoptosis was determined by TUNEL staining (D) (Left) Primary hepatocytes were isolated, treated with either TCS or DMSO, and stained with DHE. (Right) DHE fluorescence in hepatocytes was quantitated by counting positive cells in four different fields under a fluorescence microscope. (E) The up-regulation of *gp91phox*, *p47phox*, and *p67phox*, subunits of the NADPH oxidase complex, in livers of TCS-treated mice quantitated by real-time PCR.



hepatic proliferative effect through PPAR $\alpha$  activation (2). We believe that TCS modulates neither mouse nor, most likely, human PPAR $\alpha$  activation because Yang and colleagues (36) concluded that the ligand binding affinity between mouse and human PPAR $\alpha$  is very similar for general ligands by using a humanized PPAR $\alpha$  mouse model in which the human PPAR $\alpha$  gene is expressed in the *Ppara*-null background. Using a different liver carcinogenesis protocol that involves coadministration of phenobarbital, the Negishi group (8) demonstrated that CAR activation is required for liver tumorigenesis by phenobarbital. Similar to phenobarbital, TCS activates CAR through an indirect mechanism. Although TCS-mediated liver tumorigenesis occurs in both *Car*<sup>+/-</sup> and *Car*<sup>-/-</sup> mice and there is no statistical significance for tumor formation in these two groups, *Car*<sup>+/-</sup> mice had a tumor number that is nearly twice as high compared with *Car*<sup>-/-</sup> mice, indicating the possible involvement of CAR in TCS tumorigenesis. Ligand-elicited CAR activation regulates genes primarily associated with xenobiotic metabolism and steroids and bile acid homeostasis (37). Thus, TCS contamination in biological systems may pose a risk by interfering with the metabolism of endogenous and exogenous substrates through CAR-target xenobiotic genes. The link between CAR and TCS liver toxicity and the physiological effects (e.g., clinical drug–drug interactions) of TCS-mediated CAR activation need to be further identified.

In our tumorigenesis study, TCS-treated mice exhibited cell proliferation, hepatic fibrosis, and proinflammatory responses, all of which resemble the microenvironment within which human liver cancer forms (38, 39). As a weak carcinogen, DEN alone can only produce a low number of lesions that undergo malignant

conversion ~8 mo after initiation (26). Using this animal model in the 6-mo study course, we demonstrate that mice exposed to TCS markedly increased their susceptibility to tumorigenesis. HCC is the third largest cause of cancer deaths worldwide, and effective treatments have not yet emerged. We are constantly exposed to a variety of genotoxins, such as benzo(a)pyrene and heterocyclic amines, that are present in the environment and in our diet and that can potentially act as cancer initiators. Combined with the ubiquitous presence of TCS, it is expected that the manifestation of TCS-induced hepatic tumorigenesis would occur in humans as it occurs in mice. TCS is rapidly absorbed from the gastrointestinal tract and skin and is eliminated from the body mainly through glucuronidation, as evidenced by TCS glucuronides being the most abundant metabolite in urine (4). It is reasonable to speculate that, particularly when the liver is in a diseased state or UDP-glucuronyltransferase expression is not optimal (e.g., inactivating gene polymorphisms in the *UGT1A1* gene, as seen in Crigler-Najjar and Gilbert's syndromes) (40), exposure to TCS from multiple resources may exceed the metabolic capacity that the body can provide. Our results clearly document that TCS accelerates both HCC development and its long-term effects on liver damage, accompanied by fibrosis and inflammation in mice. In summary, this study provides compelling evidence that TCS plays a pathologic role in promoting tissue fibrogenesis, leading to liver carcinogenesis.

**ACKNOWLEDGMENTS.** The work was supported in part by US Public Health Service Grants ES010337 (to R.H.T., R.M.E., and M.K.), GM086713 and GM100481 (to R.H.T.), A1043477 (to M.K.), and ES0027P and ES004699 (to B.D.H.).

- McMurry LM, Oethinger M, Levy SB (1998) Triclosan targets lipid synthesis. *Nature* 394(6693):531–532.
- Rodricks JV, Swenberg JA, Borzelleca JF, Maronpot RR, Shipp AM (2010) Triclosan: A critical review of the experimental data and development of margins of safety for consumer products. *Crit Rev Toxicol* 40(5):422–484.
- Singer H, Müller S, Tixier C, Pilonel L (2002) Triclosan: Occurrence and fate of a widely used biocide in the aquatic environment: Field measurements in wastewater treatment plants, surface waters, and lake sediments. *Environ Sci Technol* 36(23):4998–5004.
- Moss T, Howes D, Williams FM (2000) Percutaneous penetration and dermal metabolism of triclosan (2,4,4'-trichloro-2'-hydroxydiphenyl ether). *Food Chem Toxicol* 38(4):361–370.
- Crofton KM, Paul KB, Devito MJ, Hedge JM (2007) Short-term in vivo exposure to the water contaminant triclosan: Evidence for disruption of thyroxine. *Environ Toxicol Pharmacol* 24(2):194–197.
- Cherednichenko G, et al. (2012) Triclosan impairs excitation-contraction coupling and Ca<sup>2+</sup> dynamics in striated muscle. *Proc Natl Acad Sci USA* 109(35):14158–14163.
- Battaller R, Sancho-Bru P, Ginès P, Brenner DA (2005) Liver fibrogenesis: A new role for the renin-angiotensin system. *Antioxid Redox Signal* 7(9–10):1346–1355.
- Ueda A, et al. (2002) Diverse roles of the nuclear orphan receptor CAR in regulating hepatic genes in response to phenobarbital. *Mol Pharmacol* 61(1):1–6.
- Yueh MF, Li T, Evans RM, Hammock B, Tukey RH (2012) Triclocarban mediates induction of xenobiotic metabolism through activation of the constitutive androstane receptor and the estrogen receptor alpha. *PLoS ONE* 7(6):e37705.
- Forman BM, et al. (1998) Androstane metabolites bind to and deactivate the nuclear receptor CAR-beta. *Nature* 395(6702):612–615.
- Yueh MF, Chen S, Nguyen N, Tukey RH (2014) Developmental onset of bilirubin-induced neurotoxicity involves Toll-like receptor 2-dependent signaling in humanized UDP-glucuronosyltransferase 1 mice. *J Biol Chem* 289(8):4699–4709.
- Chen S, Yueh MF, Evans RM, Tukey RH (2012) Pregnane-x-receptor controls hepatic glucuronidation during pregnancy and neonatal development in humanized UGT1 mice. *Hepatology* 56(2):658–667.
- Fernández MA, et al. (2006) Caveolin-1 is essential for liver regeneration. *Science* 313(5793):1628–1632.
- Parola M, Robino G (2001) Oxidative stress-related molecules and liver fibrosis. *J Hepatol* 35(2):297–306.
- Jaiswal AK (2000) Regulation of genes encoding NAD(P)H:quinone oxidoreductases. *Free Radic Biol Med* 29(3–4):254–262.
- Yamamoto Y, Moore R, Goldsworthy TL, Negishi M, Maronpot RR (2004) The orphan nuclear receptor constitutive active/androstane receptor is essential for liver tumor promotion by phenobarbital in mice. *Cancer Res* 64(20):7197–7200.
- Huang W, et al. (2005) Xenobiotic stress induces hepatomegaly and liver tumors via the nuclear receptor constitutive androstane receptor. *Mol Endocrinol* 19(6):1646–1653.
- Wei P, Zhang J, Egan-Hafley M, Liang S, Moore DD (2000) The nuclear receptor CAR mediates specific xenobiotic induction of drug metabolism. *Nature* 407(6806):920–923.
- He G, et al. (2013) Identification of liver cancer progenitors whose malignant progression depends on autocrine IL-6 signaling. *Cell* 155(2):384–396.
- Naugler WE, et al. (2007) Gender disparity in liver cancer due to sex differences in MyD88-dependent IL-6 production. *Science* 317(5834):121–124.
- Kita H, et al. (2002) Identification of HLA-A2-restricted CD8(+) cytotoxic T cell responses in primary biliary cirrhosis: T cell activation is augmented by immune complexes cross-presented by dendritic cells. *J Exp Med* 195(1):113–123.
- Seki E, et al. (2009) CCR1 and CCR5 promote hepatic fibrosis in mice. *J Clin Invest* 119(7):1858–1870.
- Kubo F, et al. (2005) Interleukin 8 in human hepatocellular carcinoma correlates with cancer cell invasion of vessels but not with tumor angiogenesis. *Ann Surg Oncol* 12(10):800–807.
- Kim SJ, et al. (2001) Expression of interleukin-8 correlates with angiogenesis, tumorigenicity, and metastasis of human prostate cancer cells implanted orthotopically in nude mice. *Neoplasia* 3(1):33–42.
- Wheeler MD, et al. (2001) The role of Kupffer cell oxidant production in early ethanol-induced liver disease. *Free Radic Biol Med* 31(12):1544–1549.
- Maeda S, Kamata H, Luo JL, Leffert H, Karin M (2005) IKKbeta couples hepatocyte death to cytokine-driven compensatory proliferation that promotes chemical hepatocarcinogenesis. *Cell* 121(7):977–990.
- Dinwiddie MT, Terry PD, Chen J (2014) Recent evidence regarding triclosan and cancer risk. *Int J Environ Res Public Health* 11(2):2209–2217.
- Hernandez-Gea V, Friedman SL (2011) Pathogenesis of liver fibrosis. *Annu Rev Pathol* 6:425–456.
- Inokuchi S, et al. (2010) Disruption of TAK1 in hepatocytes causes hepatic injury, inflammation, fibrosis, and carcinogenesis. *Proc Natl Acad Sci USA* 107(2):844–849.
- Paik YH, et al. (2014) Role of NADPH oxidases in liver fibrosis. *Antioxid Redox Signal* 20(17):2854–2872.
- Nieto N, Friedman SL, Cederbaum AI (2002) Cytochrome P450 2E1-derived reactive oxygen species mediate paracrine stimulation of collagen I protein synthesis by hepatic stellate cells. *J Biol Chem* 277(12):9853–9864.
- Battaller R, et al. (2003) NADPH oxidase signal transduces angiotensin II in hepatic stellate cells and is critical in hepatic fibrosis. *J Clin Invest* 112(9):1383–1394.
- Friedman SL (2000) Molecular regulation of hepatic fibrosis, an integrated cellular response to tissue injury. *J Biol Chem* 275(4):2247–2250.
- Tsakamoto H, Rippe R, Niemela O, Lin M (1995) Roles of oxidative stress in activation of Kupffer and Ito cells in liver fibrogenesis. *J Gastroenterol Hepatol* 10 Suppl 1:S50–S53.
- Canbay A, et al. (2003) Kupffer cell engulfment of apoptotic bodies stimulates death ligand and cytokine expression. *Hepatology* 38(5):1188–1198.
- Yang Q, et al. (2008) The PPAR alpha-humanized mouse: A model to investigate species differences in liver toxicity mediated by PPAR alpha. *Toxicol Sci* 101(1):132–139.
- Maglich JM, et al. (2003) Identification of a novel human constitutive androstane receptor (CAR) agonist and its use in the identification of CAR target genes. *J Biol Chem* 278(19):17277–17283.
- Thorgeirsson SS, Grisham JW (2002) Molecular pathogenesis of human hepatocellular carcinoma. *Nat Genet* 31(4):339–346.
- Bosch FX, Ribes J, Diaz M, Cléries R (2004) Primary liver cancer: Worldwide incidence and trends. *Gastroenterology* 127(5, Suppl 1):S5–S16.
- Tukey RH, Strassburg CP (2000) Human UDP-Glucuronosyltransferases: Metabolism, Expression, and Disease. *Annu Rev Pharmacol Toxicol* 40:581–616.